# Risks and potential benefits of adoptively transferred virus-specific T cells

Huisman, W.


BENEFITS

# CHAPTER 2

## Tracking the progeny of adoptively transferred virus-specific T cells in patients post-transplant using T-cell receptor sequencing

Wesley Huisman
Marthe C.J. Roex
Lois Hageman
Eva A.S. Koster
Sabrina A.J. Veld
Conny Hoogstraten
Peter van Balen
Esther van Egmond
Cornelis A.M. van Bergen
Hermann Einsele
Lothar Germeroth
Derk Amsen
J.H.Frederik Falkenburg
Inge Jedema

*Blood Advances 2023;*
*Vol. 7 Issue 5. Pages 812-827*

# ABSTRACT

Adoptive cellular therapies with T cells are increasingly used to treat a variety of conditions. For instance, in a recent phase I/II trial, we prophylactically administered multi-virus-specific T-cell products to protect recipients of T-cell depleted allogeneic stem-cell grafts against viral reactivations. To establish treatment efficacy, it is important to determine the fate of the individual transferred T-cell populations. However, it is difficult to unequivocally distinguish progeny of the transferred T-cell products from recipient- or stem-cell graft-derived T cells that survived T-cell depletion during conditioning or stem-cell graft manipulation. Using mRNA sequencing of the TCRβ-chains of the individual virus-specific T-cell populations within these T-cell products, we were now able to track the multiple clonal virus-specific subpopulations in peripheral blood and distinguish recipient- and stem-cell graft-derived virus-specific T cells from the progeny of the infused T-cell products. We observed in vivo expansion of virus-specific T cells that were exclusively derived from the T-cell products with similar kinetics as the expansion of virus-specific T cells that could also be detected before the T-cell product infusion. Additionally, we demonstrated persistence of virus-specific T cells derived from the T-cell products in most patients who did not show viral reactivations. This study demonstrates that virus-specific T cells from prophylactically infused multi-antigen-specific T-cell products can expand in response to antigen encounter in vivo and even persist in the absence of early viral reactivations.

# INTRODUCTION



The use of adoptive T-cell therapies has increased both in frequencies as in options in the last few decades(1). Although these strategies show promising results, it is currently difficult to adequately follow the fate of these products in the patient. *In vivo* tracking and tracing of the progeny from the infused T-cell products is vital in the assessment of treatment efficacy. For instance, when administered products fail to achieve expected results, it is important to determine whether this might be explained by lack of persistence. Likewise, selective *in vivo* expansion of the transferred T cells in response to antigen encounter would be an argument to support the case that engrafted T cells helped to elicit the clinical effect. Chapuis et al. recently tackled this by tracking adoptively transferred T-cell products using T-cell receptor (TCR) deep sequencing(2).

Patients that underwent allogeneic stem-cell transplantation (alloSCT) are (temporarily) immune-compromised and reactivations of cytomegalovirus (CMV), Epstein-Barr virus (EBV) and adenovirus (AdV) are frequently seen in these patients. The adoptive transfer of human leukocyte antigen (HLA)-matched virus-specific T cells from the original stem-cell donor can reduce viral infection and reactivation risks in these patients(3). Safety and feasibility of adoptive transfer of donor-derived virus-specific memory T-cell products has been demonstrated in multiple phase I/II clinical studies by different groups, including ours(4-12). However, persistence of the virus-specific T cells could not be attributed unequivocally to the transferred T-cell product, as T cells with the same antigen-specificity might already have been present in the patient or derived from the stem-cell graft. Furthermore, the currently used techniques (i.e. peptideMHC-tetramer staining, marker-gene analysis and/or Elispot) allow only for the detection of frequencies higher than ~0.1% within total peripheral blood mononuclear cells (PBMCs)(13-18). More sensitive and specific detection methods are required to *in vivo* track individual T-cell populations derived from the T-cell products.

In a recent phase I/II trial in our department, 24 patients who received a T-cell depleted alloSCT were treated post-transplant with a prophylactic infusion of a stem-cell donor-derived multi-(virus) antigen-specific T-cell product, containing $CD8^{pos}$ T cells directed against CMV, EBV and/or AdV antigens(19, 20). The aim was to prevent uncontrolled viral reactivations in these patients. The T cells from the products had to persist long enough without the presence of viral antigen to be able to prevent or control the viral reactivation. Safety and feasibility of this approach and appearance in peripheral blood (PB) of virus-specific T cells as detected by conventional peptide-MHC-tetramer staining were demonstrated. However, we could not determine whether these virus-specific T cells were derived from the infused product and whether virus-specific T cells persisted in those patients in which the frequencies of such cells were below the detection

threshold of conventional peptideMHC-tetramer staining.

In this study, we aimed to track prophylactically administered virus-specific T cells by using high-throughput T-cell receptor (TCR)-sequencing of the infused T-cell products and PBMC samples of the patients after administration. We analyzed in detail how many and which T cells persisted and expanded after administration of the products. Using the TCR-sequencing technology, we were able to distinguish the virus-specific T cells that were already present before infusion of the product from persisting or expanding T cells that were exclusively derived from the product.



## MATERIALS AND METHODS

**Collection of patient and donor material**

After informed consent according to the Declaration of Helsinki, PBMCs were isolated from alloSCT patients and their stem-cell donors by standard Ficoll-Isopaque separation and stored in the vapor phase of liquid nitrogen(20). The patients and donors had been included in a previous single center, phase I/II study exploring the safety, feasibility and first evidence of efficacy of prophylactic infusion of multi-antigen specific T cells to prevent complications early after T-cell depleted alloSCT(20) (T Control, EudraCT-number 2014-003171-39). Clinical results can be found in the original paper(20). In the current analysis, patients and donor-derived T-cell products were numbered identical to the phase I/II study(20). See also supplementary table 1 for relevant patient and donor characteristics.

**Generation of peptide-MHC tetramers**

All viral peptides were synthesized in-house using standard Fmoc chemistry. Recombinant HLA-A*01:01, HLA-A*02:01, HLA-A*24:02, HLA-B*07:02, HLA-B*08:01 heavy chain and human β2m light chain were in-house produced in Escherichia coli. MHC-class-I refolding was performed as previously described with minor modifications(21). Major histocompatibility complex (MHC)-class-I molecules were purified by gel-filtration using FPLC. Peptide-MHC(pMHC) tetramers were generated by labeling biotinylated pMHC-monomers with streptavidin-coupled phycoerythrin (PE; Invitrogen, Carlsbad, USA), allophycocyanin (APC, Invitrogen). Complexes were stored at -80 °C. Formation of stable pMHC-monomers was performed using UVexchange technology(22) and according to a previously described protocol(23).

**Generation of multi-antigen-specific T-cell products and isolation of single-antigen-specific T-cell populations**

T-cell products were generated using the MHC-I-Streptamer isolation technology, as

previously described(19, 20). In short, isolation complexes (MHC-I-Streptamers) were generated per target-antigen T-cell specificity. For every patient, MHC-I-Streptamers for 4 HLA*02:01-restricted viral antigens (2 CMV, 1 EBV, and 1 AdV) were pooled. In addition, depending on HLA-type of patient/donor and regardless of donor CMV, EBV, and AdV serostatus, MHC-I-Streptamers for peptides presented in HLA-A*01:01, -A*24:02, -B*07:02, and/or -B*08:01 were added to this pool (**Table 1**). The pool of MHC-I-Streptamers was incubated with $2\times10^9$ donor-derived PBMCs and MHC-I-Streptamer-bound cells were isolated using a CliniMACS Plus instrument (Miltenyi Biotec, Bergisch Gladbach, Germany) under GMP conditions. Five percent of the cells from all products, except products U (3%) and Y (4%), were non-specifically expanded using 800ng/ml phytohemagglutinin with autologous PBMCs as feeder mixture, as previously described(20), cryopreserved and used for in-depth analysis in this study. In order to isolate single-antigen-specific T-cell populations from the expanded T cells from the products, cells were first incubated with pMHC-tetramer complexes for 30 min at 4°C followed by incubation with fluorescein isothiocyanate (FITC)-labeled CD8 (BD) antibodies at 4°C for 30 min. PeptideMHC-tetramer$^{pos}$ virus-specific T cells were bulk Fluorescence Activated Cell Sorted (FACS) for each specificity and directly lysed. Sorting was performed on a FACS ARIA (BD) using Diva software (BD). For the generation of peptide-MHC-I-Tetramers, see supplementary material and methods.



**Table 1. PeptideMHC-streptamers used for the generation of multi-virus-specific T-cell products**

| Virus | Protein | Peptide | HLA-restriction | Specificity included in T-cell product manufacturing for this # patients |
|---|---|---|---|---|
| CMV | pp50 | **VTE**HDTLLY | HLA-A*01:01 | 3 |
| | pp65 | **NLV**PMVATV | HLA-A*02:01 | 20 |
| | IE1 | **VLE**ETSVML | HLA-A*02:01 | 20 |
| | pp65 | **QYD**PVAALF | HLA-A*24:02 | 6 |
| | pp65 | **TPR**VTGGGAM | HLA-B*07:02 | 7 |
| | IE1 | **QIK**VRVDMV | HLA-B*08:01 | 5 |
| EBV | BMLF1 | **GLC**TLVAML | HLA-A*02:01 | 20 |
| | EBNA3A | **RPP**IFIRRL | HLA-B*07:02 | 7 |
| | BZLF1 | **RAK**FKQLL | HLA-B*08:01 | 5 |
| AdV | HEXON | **TDL**GQNLLY | HLA-A*01:01 | 3 |
| | E1A | **LLD**QLIEEV | HLA-A*02:01 | 20 |
| | HEXON | **TYF**SLNNKF | HLA-A*24:02 | 6 |
| | HEXON | **KPY**SGTAYNAL | HLA-B*07:02 | 7 |

Abbreviations: CMV, Cytomegalovirus. EBV, Epstein Barr virus. AdV, Adenovirus

**TCRβ-library preparation**

TCRβ-sequences were identified using ARTISAN PCR adapted for TCR PCR as previously described(24-26). Ten µl (~1µg) of mRNA per sample was mixed with TCRβ constant region-specific primers (1µM final concentration) and SmartSeq2modified template-switching oligonucleotides (SS2m_TSO; 0.2µM final concentration) and denatured for 3 minutes at 72°C. After cooling, cDNA was synthesized for 90 minutes at 42°C with 170U SMARTscribe reverse transcriptase (Takara, Clontech) in a total volume of 20µl containing 1.7U/µl RNasin (Promega), 1.7mM DTT (Invitrogen, Thermo Fisher Scientific), 0.8mM each of high-purity RNAse-free dNTPs (Invitrogen, Thermo Fisher Scientific) and 4µl of 5x first-strand buffer. During cDNA synthesis, a non-templated 3'polycytosine terminus was added, which created a template for extension of the cDNA with the TSO(24). PCR (2min at 98°C followed by 40 cycles of [1s at 98°C, 15s at 67°C, 15s at 72°C], 2 min at 72°C) of 5µl of cDNA was then performed using Phusion Flash (Thermo Fisher Scientific) with anchor-specific primer (SS2m_For; 0.4µM final concentration) and each (0.4µM final concentration) of the nested primers specific for the constant regions of TCRβ constant 1 and TCRβ constant 2. Both forward and reverse PCR primers contained overhanging sequences suitable for barcoding. Amplicons were purified and underwent a second PCR (2min at 98°C followed by 10 cycles of [1s at 98°C, 15s at 65°C, 30s at 72°C], 2 min at 72°C) using forward and reverse primers (0.5µM final concentration) with overhanging sequences containing identifiers (sequences of 6 base-pairs) and adapter sequences appropriate for Illumina HiSeq platforms or Novaseq. See supplementary tables 2 and 3 for primer and identifier sequences, respectively. Total mRNA (10µl) was extracted from T cells from 20 unsorted products and 81 pMHC-tetramer$^{pos}$ CD8$^{pos}$ T-cell populations directly after FACSorting using magnetic beads (Dynabead mRNA DIRECT kit: Invitrogen, Thermo Fisher Scientific) (**Supplementary Figure 1A**). To investigate whether T cells with TCRβ-sequences detected in the T-cell products were present in PB of the patients after administration, we isolated primary CD8$^{pos}$ T cells from follow-up PB samples with magnetic activated cell sorting (MACS) using CD8 T-cell isolation kits with LS columns from Miltenyi Biotec (Bergisch Gladbach, Germany). Peripheral blood samples at moment of product infusion contained a median of 110*10$^6$ CD8$^{pos}$ T cells/L (Inter quartile range IQR: 47-509, **Supplementary Figure 2A**). After CD8 enrichment all PB samples contained a median of 81% CD8$^{pos}$ cells (IQR: 61%-92%, **Supplementary Figure 2B**) PB samples for follow-up were taken every 2 weeks until 8 weeks after T-cell product infusion and every 4 weeks thereafter until 6 months after alloSCT(20). Total mRNA (10µl) was extracted from 109 CD8$^{pos}$ populations isolated from follow-up PB samples of the patients (**Supplementary Figure 1B**), containing a median of 0.3*10$^6$ cells (IQR 0.16-0.66*10$^6$ cells, **Supplementary Figure 2C**). The samples from each patient were sequenced separately. Unique identifiers were used for the PCR products of each virus-specific T-cell population, unsorted T-cell product and each monitoring sample (see **Supplementary Tables 2 and 3** for primer and identifier sequences, respectively).

These amplicons with identifiers were purified, quantified and pooled into one library per patient for paired-end sequencing of 125bp on an Illumina HiSeq4000 or Novaseq 6000. The samples of each patient were separately sequenced on different chips to obtain enough reads per sample (oversampling). Each $CD8^{pos}$ PB follow-up sample contained a median of $8.5*10^6$ reads (IQR 5.5-12.8*$10^6$ reads, **Supplementary Figure 2D**). Because of the oversampling this resulted in a median of 28 reads per cell per sample (IQR 14-46 reads per cell, **Supplementary Figure 2E**). Deep sequencing was performed at GenomeScan (Leiden, The Netherlands) and almost all reads contained a Phred quality score above Q30 (median 92%, IQR 90%-93%). One-third of a lane (~100.000.000 reads) was used per library while the other lanes were used for other projects that did not contain TCR-sequences. Raw data was de-multiplexed and aligned to the matching T-cell receptor beta variable (TRBV), diversity (TRBD), joining (TRBJ) and constant (TRBC) genes. In total, a median of 33% (IQR 22%-49%) of all reads could successfully be aligned, **Supplementary Figure 2F**). CDR3β-sequences were built using MIXCR software using a bi-directional approach (5'-3' and 3'-5' read)(27). MIXCR corrects for PCR and sequencing errors (https://mixcr.readthedocs.io/en/master/). CDR3β-sequences that were present in multiple T-cell populations with different specificities as a result of FACS contamination, were annotated to the T-cell population that contained this sequence more than 10-fold compared to the other T-cell populations with different specificities (Representative example, **Supplementary Figure 3**). An exception was made for dominant T-cell populations that contained one or two CDR3β-sequences that were present at high frequencies (>40%) within this T-cell population and at high frequencies within the total product. Such sequences contaminated T-cell populations that were of low frequency within the product. This was only the case for CDR3β-sequences specific for CMV-$pp65^{TPR}$, CMV-$pp50^{VTE}$, EBV-$EBNA3A^{RPP}$, and EBV-$BZLF1^{RAK}$ from products F, T, Y and V, respectively. In these cases, a 5-fold difference in frequency compared to T-cell populations with other specificities was used for annotation.

**Target-antigen-specific immune reconstitution**

Absolute numbers of circulating $CD3^{pos}$/$CD8^{pos}$ T cells per liter blood were determined on fresh blood by flow cytometry. Absolute numbers of circulating $CD4^{pos}$ T cells ($CD45^{pos}CD3^{pos}CD4^{pos}$), $CD8^{pos}$ T cells ($CD45^{pos}$ $CD3^{pos}CD8^{pos}$), B cells ($CD45^{pos}CD3^{neg}CD19^{pos}$) and NK cells ($CD45^{pos}CD3^{neg}CD16/CD56^{pos}$ cells) were determined as part of routine clinical evaluation on fresh venous blood using BD TruCount Tubes (BD), following the manufacturer's instructions. Samples were stained with APC-labeled CD3 (BD), FITC-labeled CD4 (BD), PE-labeled CD8 (BD), PerCP-labeled CD45 (BD) or with FITC-labeled CD3 (BD), PE-labeled CD16 (BD), APC-labeled CD19 (BD), PerCP-labeled CD45 (BD) and PE-labeled CD56 (BD). Cells were measured on a FACS Canto and analyzed using Diva Software. Frequencies of target-antigen-specific T cells were determined based on the percentages of target-antigen-specific TCR-nucleotide-sequences from each $CD8^{pos}$

populations isolated from a follow-up sample. Absolute numbers of target-antigen-specific T cells per liter were calculated by multiplying the percentages of target-antigen-specific TCR-nucleotide-sequences, with the absolute numbers of $CD3^{pos}CD8^{pos}$ T cells per liter blood.



**Detection limit and cut-off value**

A median of $3.7*10^5$ (range $0.6\text{-}74*10^5$) and a median of $3.6*10^5$ (range $1.2\text{-}47*10^5$) $CD8^{pos}$ T cells were MACS isolated from PB for each patient before infusion of the T-cell product and from subsequent monitoring samples, respectively. In theory we could detect the amplified reads from one T cell. One T cell would correspond with a median frequency of 0.0037% and 0.0036% for samples before and after infusion of the product, respectively. Due to this detection limit, we used a cut-off whereby sequences were analyzed that occurred at frequencies above 0.001%, while sequences below this frequency were not analyzed.

## RESULTS

**Annotation and quantification of virus-specific T-cell receptor sequences from the T-cell products**

In a recent phase I/II trial, 24 stem-cell donor-derived multi-(virus)antigen-specific T-cell products, each containing $CD8^{pos}$ T-cell populations specific for several CMV, EBV and AdV antigens, were generated and prophylactically administered to the respective patients early after T-cell depleted alloSCT(20). All donors were EBV seropositive, 13 donors were CMV seropositive, whereas the serostatus for AdV was not determined (Supplementary table 1). All products contained EBV-specific T cells, all but one contained AdV-specific T cells, whereas CMV-specific T cells were only detectable in products from CMV-seropositive donors. We aimed to track the *in vivo* fate of the transferred virus-specific T cells through high-throughput TCR-sequencing of virus-specific T cells from the products and of $CD8^{pos}$ T cells in PB samples of the patients taken at different times after infusion of the products. In order to track these T cells, TCR-sequences had to be correctly allocated to the virus-specific T-cell populations that were present in each product. To this end, T-cell products were first polyclonally expanded *in vitro* to have sufficient T cells to sort each virus-specific T-cell population and to allocate the TCR-sequences to the specific populations (for a schematic overview see: **Supplementary Figure 1A**). Insufficient PB samples were available from two patients, which were therefore excluded from analysis. Additionally, T cells of two T-cell products could not be expanded *in vitro* and thus the patients that had received the corresponding T-cell products were also excluded from analysis. From 20 out of the initial 24 products, a median of $0.29*10^6$ T cells were expanded to a median of $21.9*10^6$ T cells (**Figure 1A**). From these expanded

fractions, we separately isolated all the different virus-specific T-cell populations that were present in each product(20) by FACS using pMHC-tetramers and performed TCR-sequencing of the CDR3β-regions of each isolated virus-specific T-cell population. Unsorted fractions of the expanded T-cell products were also sequenced in parallel to quantify the different virus-specific TCRs present in the products (**Supplementary Figure 1A**). In total, 97.5% (range 81%-100%) of the TCR-sequences from the sorted virus-specific T-cell populations could be detected in the unsorted bulk products (data not shown). To investigate the distribution of the different specificities in each product, we analyzed the frequencies of the TCR-sequences for each target-antigen of each virus. In total, from the 13 products that were generated from CMV-seropositive donors, TCRs of 32 CMV-specific T-cell populations were annotated (**Figure 1B**). From the 20 products (all of which were generated from EBV-seropositive donors), TCRs of 31 EBV-specific T-cell populations were annotated (**Figure 1C**). Finally, we could annotate the TCRs of a total of 22 AdV-specific T-cell populations from 17 expanded products (**Figure 1D**), whereas 2 expanded products yielded insufficient numbers of AdV-specific cells after expansion for analysis.



To investigate how many different clonal virus-specific T-cell populations from each product we could potentially track *in vivo*, we quantified the different TCR-nucleotide sequences for each virus-specific T-cell population within the T-cell products. The CMV-, EBV-, or AdV-specific T-cell populations from the products contained a median of 30 (range 1-79), 34 (range 5-140) and 20 (range 2-74) different TCR-nucleotide sequences, respectively (**Figures 1E, 1F and 1G**). The majority of virus-specific TCR-nucleotide sequences were found at low frequencies (between 0.001% and 0.1%) in these expanded T-cell products (**Supplementary Figure 4**).

**T cells with TCR-nucleotide sequences found in the T-cell products could be identified in patients with and without detectable viral-loads**

To investigate whether virus-specific T cells from the infused T-cell products could be found back in PB samples of the patients, we sequenced the TCRs of $CD8^{pos}$ T-cell fractions from PB samples taken at various timepoints after infusion of the T-cell products (see Supplementary Figure 2 for sample quality assessments). These TCR-nucleotide sequences were then compared with the TCR-nucleotide sequences that were present in the T-cell products (for a schematic overview see: **Supplementary Figure 1B**).

We previously illustrated that despite T-cell depletion of the graft, part of the donor-derived T-cell compartment can survive this procedure(28, 29). This implies that TCRs detected in post-infusion samples may not necessarily be derived from the infused products, but may have already been introduced in the patients with the stem-cell grafts. We therefore also analyzed PB samples that were obtained from patients before infusion

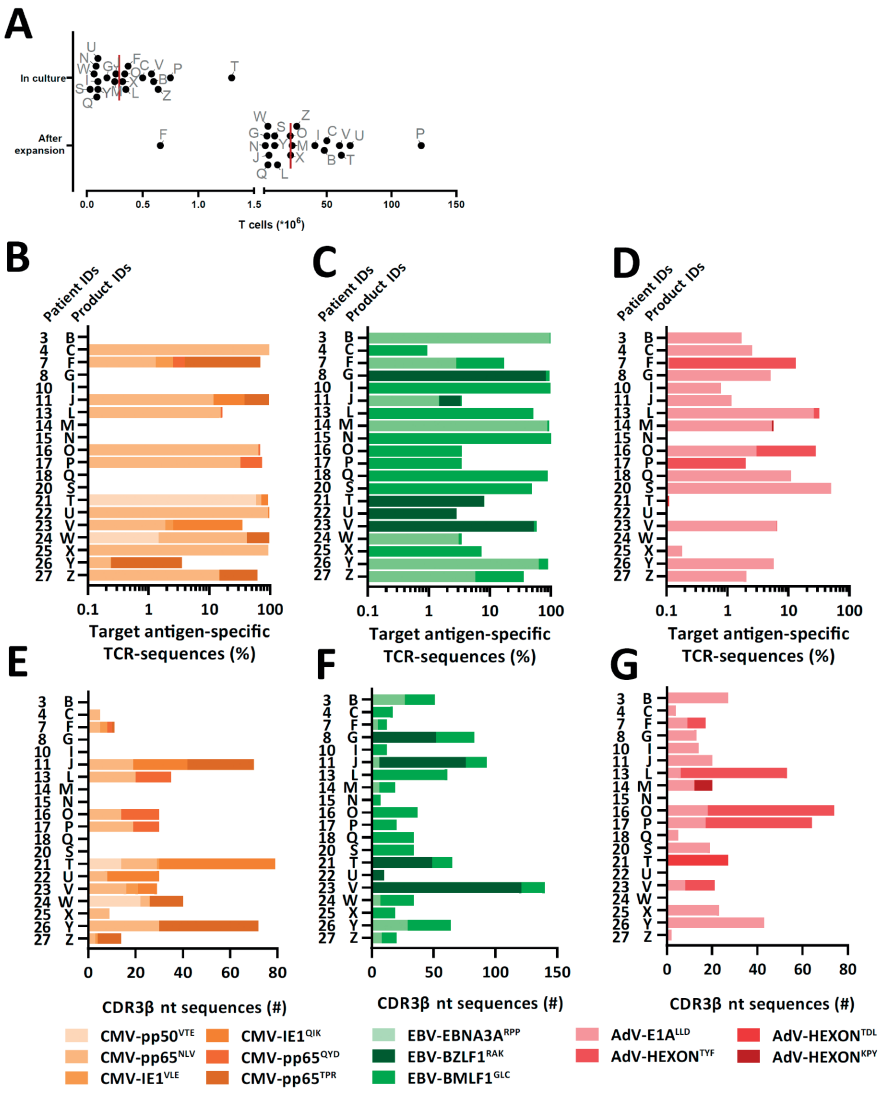


**Figure 1. Annotation and quantification of virus-specific TCR-sequences from the T-cell products.**
T cells from 20 T-cell products were successfully expanded. The different virus-specific T-cell populations were FACSorted from these expanded products into separate pure populations using pMHC-tetramers followed by direct mRNA isolation and TCR-sequencing of the CDR3β-regions. The remaining unsorted T cells from the T-cell products were sequenced in parallel to quantify the TCRs that were present in the products. **A)** The numbers of T cells from the products that were put in culture and the cell numbers after expansion are shown. The red-lines represent medians. **B, C and D)** Shown are the frequencies of CMV **(B)**, EBV **(C)** and AdV **(D)** –specific TCR-nucleotide sequences (CDR3β-sequences) that were present in the target-antigen-specific T-cell products. The sum of all target-antigen-specific TCR-nucleotide sequences were set to 100%. The different virus-specificities are shown as stacked-columns for each product. **E, F and G)** The number of different CDR3β-sequences are shown that were specific for CMV (**E**), EBV **(F)** and AdV **(G)**-derived antigens for each product.
Abbreviations: CMV, Cytomegalovirus. EBV, Epstein Barr virus. AdV, Adenovirus. CDR3, complementary determining region 3. nt, nucleotide

of the products. In figure 2 we separately depicted the virus-specific TCR-nucleotide sequences present in the products that could be found in patient PB samples only after infusion (orange: CMV, green: EBV and red: AdV), both before and after infusion (light orange: CMV, light green: EBV and light red: AdV), or could not be found after infusion (white) (**Figures 2A, 2B and 2C**). In addition, we determined whether the diversity (number of different TCR-nucleotide-sequences) correlated with viral reactivation as determined by presence of viral-load in PB.



In 9 patients the presence of some CMV-specific T-cell populations could not unequivocally be ascribed to the infused T-cell product, as the same sequences were also found in PB samples taken before infusion (**Figure 2A**, light orange bars). However, many CMV-specific TCR-nucleotide sequences were only found in PB samples of the 13 patients after infusion, strongly indicating that they originated from the infused products (**Figure 2A,** orange bars). Such TCRs were found both in patients with or without viral-load after infusion and a higher number of different TCRs (diversity) were found in samples from patients with CMV reactivations than in samples from patients without CMV reactivations following infusions, indicating *in vivo* expansion in response to the virus (**Figure 2D**). Similar results were obtained for the EBV-specific T-cell populations (**Figure 2B**). In 13 patients, a number of EBV-specific TCR-nucleotide sequences were found both before and after infusion. Conclusions about their origin from the infused products (light green bars) could therefore not be made. However, in 16 patients TCR-nucleotide sequences of EBV-specific T cells could be tracked in PB samples only after infusion of the products (green bars) and these EBV-specific TCRs were more abundant in patients with EBV reactivations than in those without (**Figure 2E**). In 2 patients without EBV reactivation, EBV-specific TCR-nucleotide sequences from the infused products could not be detected in the PB samples. Finally, while PB samples from 6 patients contained AdV-specific TCR-nucleotide sequences that were present also in the patients prior to infusion, in 8 patients AdV-specific TCR-nucleotide sequences were found in samples only after infusion of the products (**Figure 2C**, red bars). In PB samples of the single patient with a single positive AdV viral-load, no AdV-specific TCRs could be tracked back. These data show that after infusion of the multi antigen-specific T-cell products, in most patients high frequencies of virus-specific TCRs could be identified that were derived from the infused T-cell products. As measured by frequencies of virus-specific TCRs, significantly larger proportions of the T-cell products were found back in patients with viral reactivations compared to patients without viral reactivations, indicating that these virus-specific T cells from the T-cell products contributed to the anti-viral immune response.

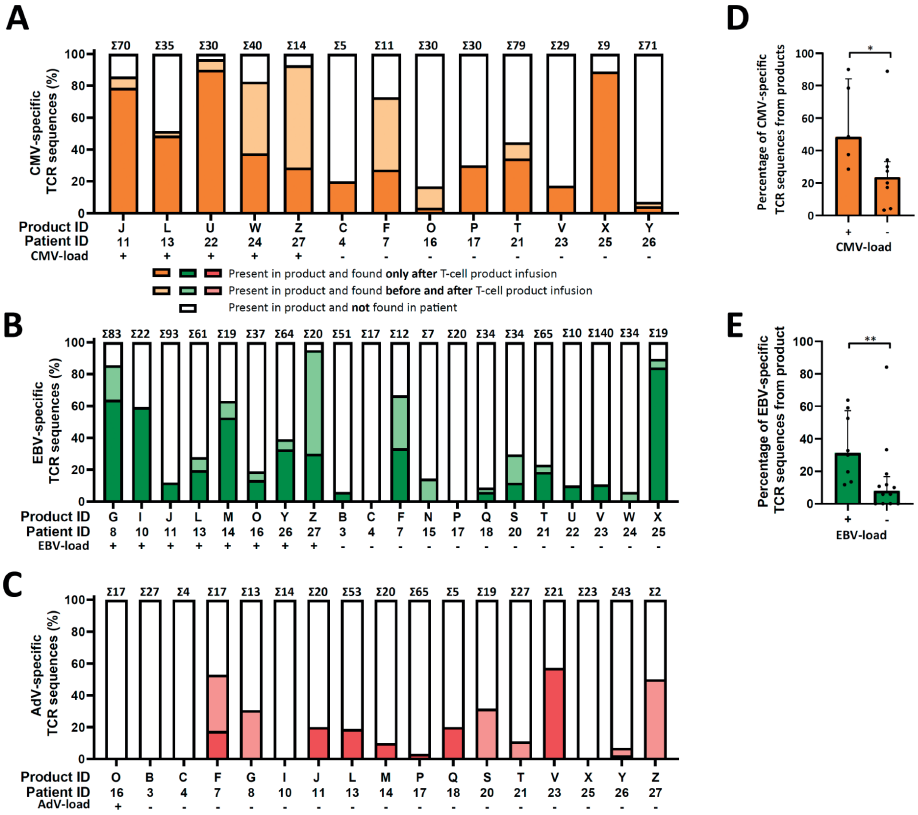


**Figure 2. Virus-specific T cells with TCR-nucleotide sequences found in the T-cell products, could be identified in patients with and without detectable viral-loads.** The total numbers (Σ) of different virus-specific TCR-nucleotide sequences are shown for each product (above each bar). Patients are grouped according to detectable viral-loads after infusion of the T-cell product. **A, B and C**) Shown are the percentages of different CMV- (**A**) , EBV- (**B**) and AdV- (**C**) specific TCR-nucleotide sequences that could be found back only after infusion of the products (color-scale), be detected before and after infusion (light-color-scale) or not detected (white). **D and E)** The numbers of different TCR-nucleotide sequences that were found only after infusion, shown as percentages in barplots with the median and inter-quartile range, were compared between patients with and without CMV viral-load (**D**) and with and without EBV viral-load (**E**).
Statistical differences were assessed with the Mann-Whitney t test (D and E). *P< .05; **P < .01.

## Kinetics of virus-specific T cells with TCR-nucleotide sequences from the infused products in patients with and without viral-loads after infusion

For a number of T-cell populations it was impossible to tell on the basis of TCR-sequence detection alone to what extent their presence was explained by infusion of the T-cell product, given that they were already present in the patients prior to infusion. However, we reasoned that we might still be able to assess the contribution of transfused T cells to viral control by examining their expansion kinetics after infusion of the T-cell

product. If T cells derived from the product would significantly contribute to controlling the virus, we hypothesized that irrespective of their presence or absence in the patient prior to infusion, similar kinetics of the progeny of the virus-specific T-cell populations from the products should be found. Virus-specific T cells would show expansion in case of reactivation and only persistence in the absence of viral-load after infusion. We therefore investigated the kinetics of virus-specific T-cell populations that appeared after infusion of T-cell products in patients with and without viral reactivations (colored) and compared these with the kinetics of virus-specific T-cell populations that were present prior to product infusion (grey). In figures 3, 4 and 5 we separately depicted the kinetics of CMV, EBV and AdV-specific T-cell populations (with TCR-nucleotide sequences that were found in the products) in the presence and absence of viral-loads after infusion.



**CMV**

As illustrated in figures 3A and 3B, positive CMV viral-loads were detected in 5 out of 13 patients before and after infusion of the T-cell products. In 4 of these 5 patients, CMV viral-loads were also detected at the moment of infusion of the T-cell products. In all 5 patients, CMV-specific TCR-nucleotide sequences that only appeared after infusion and those that were present already before infusion of the T-cell products exhibited similar expansion and contraction that correlated with the increase and decrease of viral-loads (**Figure 3A and 3B**). The responding individual CMV-specific T-cell clones all showed similar expansion kinetics, including T-cell clones that contained public TCRs (TCR-amino-acid sequences that are identical in different individuals) as well as T-cell clones containing private TCRs (**Supplementary Figure 5A and 5B**). During follow-up of the other 8 patients, no CMV viral-loads were detected after infusion. Two patients (patients 7 and 16) had positive CMV viral-loads, which had been cleared before infusion of the products (data not shown). In all 8 patients we detected T cells with CMV-specific TCR-nucleotide sequences from the products that only appeared after infusion and persisted without clear expansions in 6 out of 8 patients (**Figure 3C**). In 4 of these patients, we also detected CMV-specific TCR-nucleotide sequences that were present before and after infusion of the T-cell products showing similar kinetics (**Figure 3D**).

**EBV**

As shown in figures 4A and 4B, reactivations, as reflected by positive EBV viral-loads, were detected in 8 out of 20 patients after infusion of the T-cell products. Detectable EBV viral-loads were absent in all 8 patients at the time of T-cell product infusions, but EBV viral-loads had been detected before infusion in 3 out of 8 patients (patients 11, 13 and 26: data not shown). In all 8 patients, EBV-specific TCR-nucleotide sequences that only appeared after infusion and EBV-specific TCR-nucleotide sequences that were present before and after infusion of the T-cell products showed similar expansion and contraction that correlated with the increase and decrease of viral-loads (**Figure**

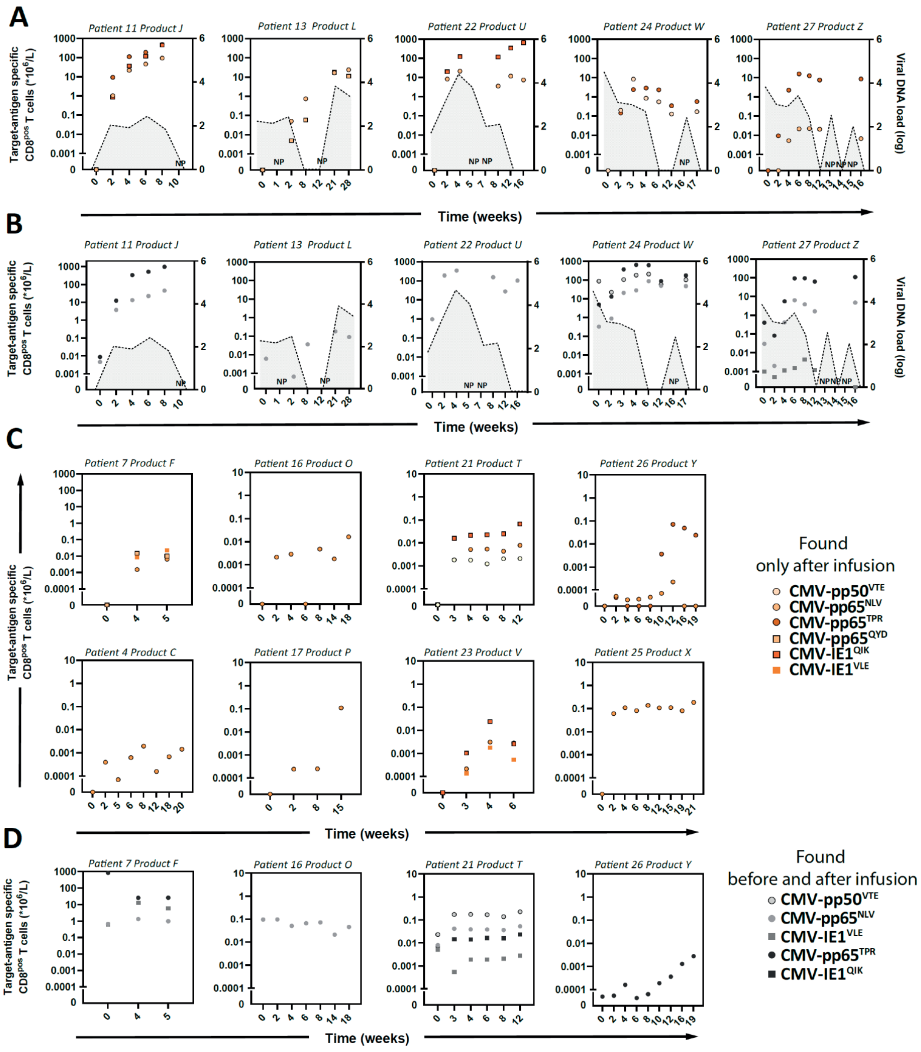


**Figure 3. Kinetics of CMV-specific T cells with TCR-nucleotide sequences also present in the infused T-cell products in patients with and without viral-loads after infusion.** Positive CMV viral-loads were detected in 5 out of 13 patients that received a T-cell product containing CMV-specific T cells. PB samples that were obtained before and after infusion of the products were MACSorted for $CD8^{pos}$ T cells followed by mRNA isolation and sequencing of the TCRs. The numbers of target-antigen specific $CD8^{pos}$ T cells/L blood were calculated by multiplying the frequencies of CMV-specific TCR-nucleotide sequences with the absolute numbers of $CD3^{pos}/CD8^{pos}$ T cells per liter. CMV viral-loads (dashed lines with grey area under the curve) and absolute numbers of CMV target-antigen-specific T cells in PB samples are illustrated from the moment just before product infusion (day 0) until the end of follow-up. **A and B**) Shown are the kinetics of CMV target-antigen-specific T cells in patients with CMV-reactivations where TCR-nucleotide sequences were found that only appeared after infusion of the products (**A**) and appeared before and after infusion of the products (**B**). **C and D)** Shown are the kinetics of CMV target-antigen-specific T cells in patients without detectable CMV viral-loads where TCR-nucleotide sequences that were identical to the products were found that only appeared after infusion of the products (**C**) and appeared before and after infusion of the products (**D**).
Abbreviations: NP, (TCR-sequencing) Not Performed.

**4A and 4B**). Individual EBV-specific T-cell clones all showed similar expansion kinetics, including T-cell clones that contained public TCRs and T-cell clones containing private TCRs (**Supplementary Figure 5C and 5D**). During follow-up of the other 12 patients, no EBV viral-loads were detected after infusion, but EBV viral-loads had been detected before infusion in 2 out of 12 patients (patients 3 and 23: data not shown). In 8 out of 12 patients we detected EBV-specific TCR-nucleotide sequences from the products that only appeared after infusion, showing persistence without clear expansions in 5 out of 8 patients (**Figure 4C**). In 5 patients, we also detected T cells with EBV-specific TCR-nucleotide sequences that were present before and after infusion of the T-cell products, showing similar kinetics in all patients, except for patient 25 (**Figure 4D**).



**AdV**

One out of 17 patients (patient 16) who was prophylactically infused with a product that contained AdV-specific T cells, showed a detectable AdV viral-load at week 16 post infusion. AdV-E1A$^{LLD}$ and AdV-HEXON$^{TYF}$-specific T cells were present in T-cell product P, but no AdV-specific TCR-nucleotide sequences could be detected in the PB samples before or after infusion of the product. During follow-up of the other 16 patients, AdV viral-loads were undetectable after infusion of the products. In 8 out of 16 patients, we detected T cells with AdV-specific TCR-nucleotide sequences from the products that only appeared after infusion, showing persistence without clear expansions in 7 out of 8 patients (**Figure 5A**). In 2 of these patients, we also detected T cells with AdV-specific TCR-nucleotide sequences that were present before and after infusion of the T-cell products showing similar kinetics, except for patient 26 (**Figure 5B**).

Based on these results, we conclude that in 5/5 patients with a detectable CMV viral-load and in 8/8 patients with a detectable EBV viral-load, T cells with CMV and EBV-specific TCR-nucleotide sequences that were only found after infusion of the products displayed similar kinetics as those that were found before and after infusion of the products. One patient had a detectable AdV viral-load during follow-up, but no T cells with AdV-specific TCR-nucleotide sequences could be detected. In 8/8 patients without detectable CMV viral-loads, 8/12 patients without detectable EBV viral-loads and in 8/16 patients without AdV viral-loads, persistence of CMV, EBV and AdV-specific T cells with TCR-nucleotide sequences that were found in the products were observed, which were not detected before infusion.

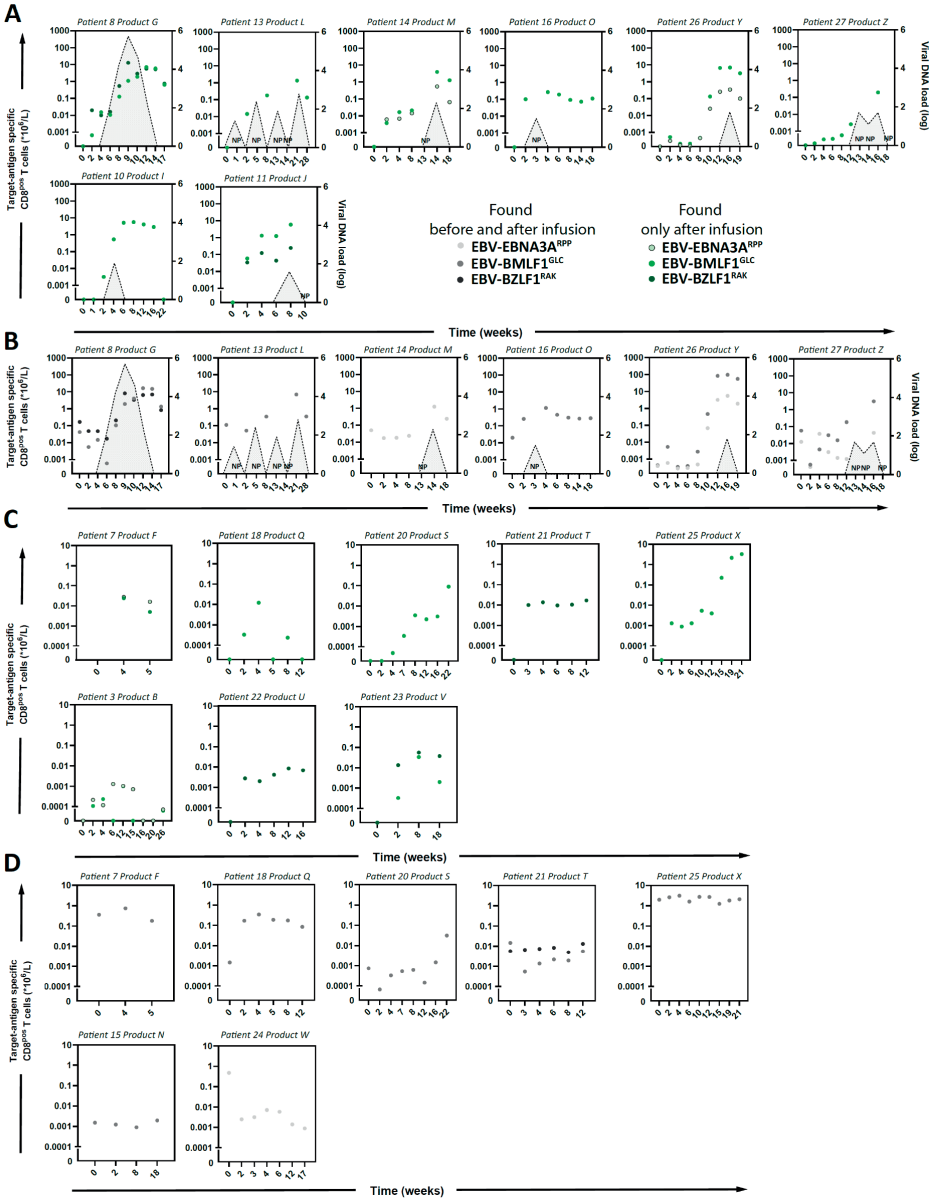


**Figure 4. Kinetics of EBV-specific T cells with TCR-nucleotide sequences present in the infused T-cell products in patients with and without viral-loads after infusion.** Positive EBV viral-loads were detected in 8 out of 20 patients that received a T-cell product containing EBV-specific T cells. PB samples that were obtained before and after infusion of the product were MACSorted for $CD8^{pos}$ T cells followed by mRNA isolation and sequencing of the TCRs. The numbers of target-antigen specific $CD8^{pos}$ T cells/L blood were calculated by multiplying the frequencies of EBV-specific TCR-nucleotide sequences with the absolute numbers of $CD3^{pos}CD8^{pos}$ T cells per liter blood. EBV viral-loads (dashed lines with grey area under the curve) and absolute numbers of EBV target-antigen-specific T cells in PB samples are illustrated from the moment just before product infusion (day 0) until the end of follow-up. **A and B**) Shown are the kinetics of EBV target-antigen-specific T cells in patients with EBV-reactivations where TCR-nucleotide sequences were found that only appeared after infusion of the products (**A**) and appeared before and

after infusion of the products (**B**). **C and D)** Shown are the kinetics of EBV target-antigen-specific T cells in patients without detectable EBV viral-loads where TCR-nucleotide sequences that were identical to the products were found that only appeared after infusion of the products (**C**) and appeared before and after infusion of the products (**D**).
Abbreviations: NP, (TCR-sequencing) Not Performed.



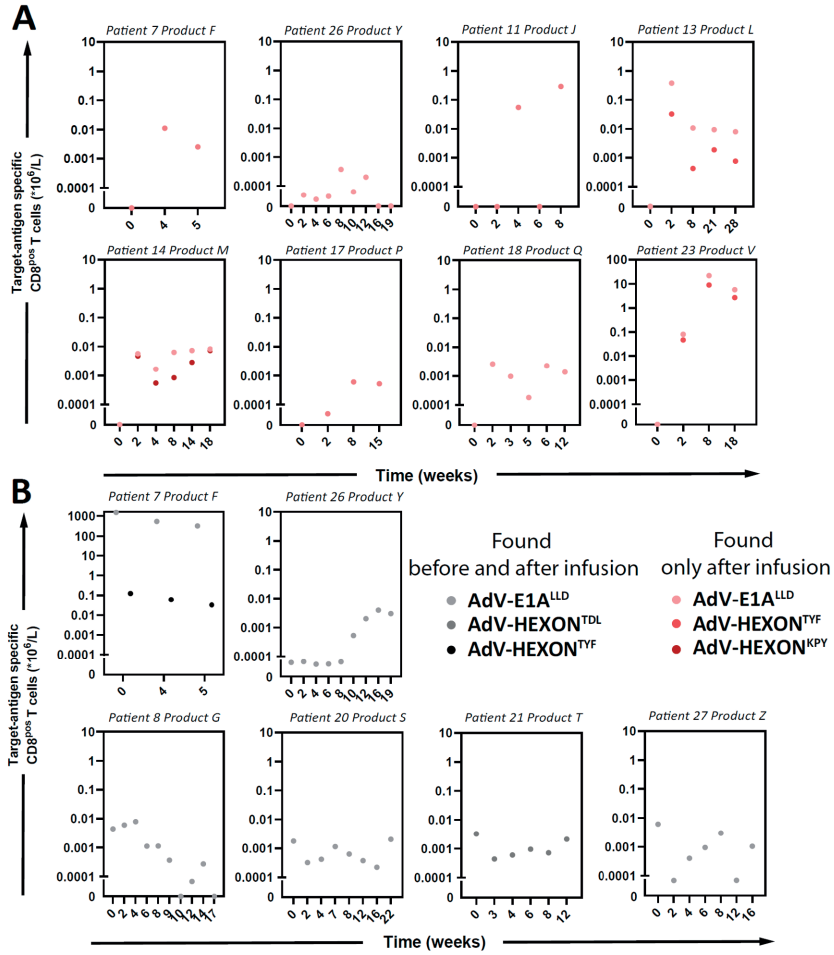


**Figure 5. Kinetics of AdV-specific T cells with TCR-nucleotide sequences present in the infused T-cell products in patients without viral-loads after infusion.** In 16 out of 17 patients that received a product that contained AdV-specific T cells no AdV viral-load was detected after infusion of the product. Peripheral blood samples of these 16 patients that were obtained before and after infusion of the product were MACSorted for $CD8^{pos}$ T cells followed by mRNA isolation and sequencing of the TCRs. The numbers of target-antigen specific $CD8^{pos}$ T cells/L were calculated by multiplying the frequencies of AdV-specific TCR-nucleotide sequences with the absolute numbers of $CD3^{pos}CD8^{pos}$ T cells per liter blood. Absolute numbers of AdV target-antigen-specific T cells in peripheral blood samples are illustrated from the moment just before product infusion (day 0) until the end of follow-up. **A and B)** Shown are the kinetics of AdV target-antigen-specific T cells in patients without detectable AdV viral-loads where TCR-nucleotide sequences that were identical to the products were found that only appeared after infusion of the products (**A**) and appeared before and after infusion of the products (**B**).
Abbreviations: NP, (TCR-sequencing) Not Performed.

**Longitudinal analysis of total numbers of product-derived CMV and EBV-specific T cells**

To study the association between viremia and the kinetics of expansion/persistence of adoptively transferred CMV- and EBV-specific T cells, we performed statistical modeling. First, we compared the smoothened Loess curves of the kinetics of all product-derived CMV- and EBV-specific T cells for patients with viral-loads and patients who never had detectable viral-loads during follow-up after product infusion. As expected, product-derived CMV-specific T cells that were only detected after product infusion showed more vigorous expansion in patients with CMV viral-loads during follow-up (Orange solid line) compared to patients who never had detectable CMV viral-loads (Orange dashed line; **Figure 6A**). Product-derived CMV-specific T cells that were detected before and after infusion followed a similar pattern, with more expansion in patients with CMV viral-loads (Grey solid line) than patients without CMV viral-loads (Grey dashed line; **Figure 6B**). Product-derived EBV-specific T cells that were only detected after product infusion showed the same pattern as CMV-specific T cells, with more expansion in patients with EBV viral-loads (Green solid line) compared to patients without EBV viral-loads (Green dashed line; **Figure 6C**). Similar trends were found for EBV-specific T cells that were detected before and after infusion (**Figure 6D**). To investigate whether the increases in numbers of CMV and EBV-specific T cells were indeed significantly associated with viremia, we constructed 4 linear mixed models with the presence of viral-load as a time-dependent covariate. The models contained two fixed effects, being time since infusion in weeks and whether or not the measurement was taken after the first appearance of viral-load (per patient). For the modeling of product-derived T cells that were found only after infusion, a patient-specific random slope effect for time was included to account for the heterogeneity in the trajectories between patients. For the modeling of product-derived T cells that were found before and after infusion, also a random intercept effect was added, since the T cells were already detectable at time of infusion. For CMV, the start of detectable viral-loads was significantly associated with higher T-cell numbers ($p=<0.0001$ and $p=0.0001$ for T cells found only after infusion and T cells found before and after infusion, respectively). Similarly, the appearance of EBV viral-loads was significantly associated with higher numbers of EBV-specific T cells that were found only after infusion ($p=<0.0001$), but a nonsignificant association ($p=0.1771$) with viral-load was observed for EBV-specific T cells that were found before and after infusion. These data show that the in-vivo expansion/persistence kinetics of adoptively transferred CMV- and EBV-specific T cells that were only detected after infusion were significantly different for patients with viral-loads (strongly expanding/proliferating) compared to patients that did not develop detectable viral-loads in the follow-up period after T-cell product infusion (persisting/maintenance).

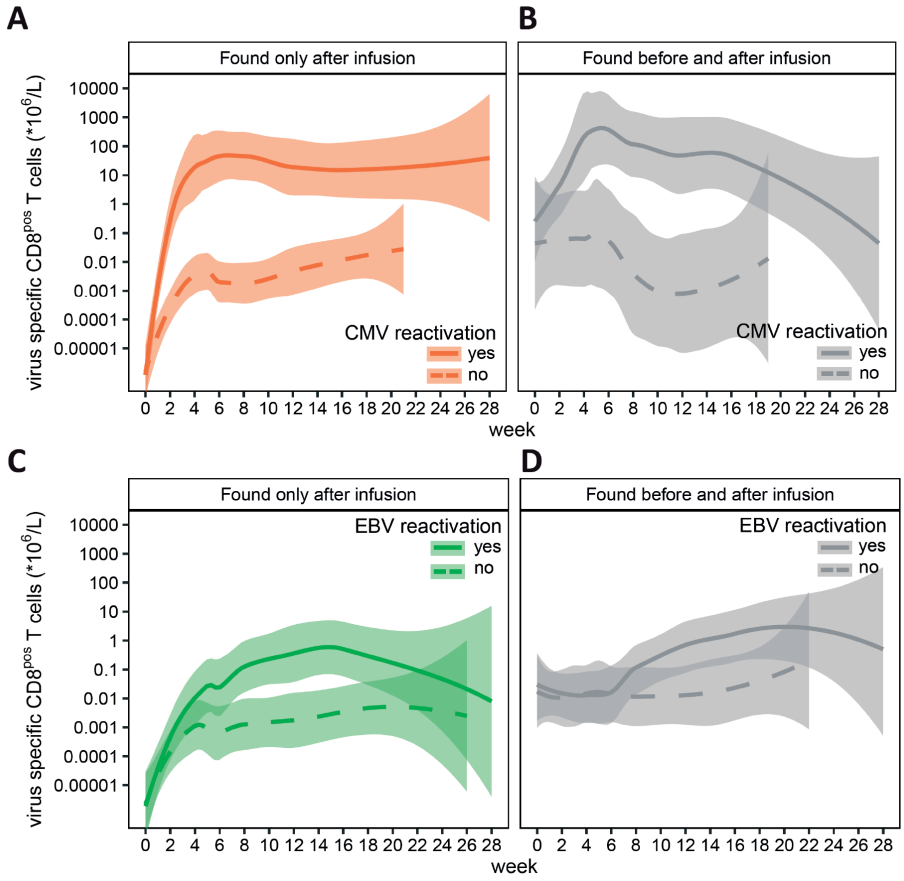


**Figure 6. Statistical modeling of the expansion/persistence kinetics of adoptively transferred CMV and EBV-specific T cells and the presence of viral-loads in the follow-up period after T-cell product infusion.** Positive CMV or EBV viral-loads were detected after infusion of T-cell products in 5 out of 13 patients and 8 out of 20 patients that received a T-cell product containing CMV-or EBV-specific T cells, respectively. Smoothed Loess curves were plotted to study the association between viremia and expansion/persistence kinetics of adoptively transferred CMV- and EBV-specific T cells. **A and B**) Kinetics of the numbers of product-derived CMV-specific T cells that were only detected after T-cell product infusion (A) or both before and after infusion (B) are shown for patients with a positive CMV viral-load during follow-up (solid line) and without detectable viral-loads in the follow-up period (dashed line). **C and D**) Product-derived EBV-specific T cells that were only detected after infusion (**C**) or both before and after infusion (**D**) are shown for patients with a positive EBV viral-load during follow-up (solid line) and without detectable viral-loads (dashed line).

## DISCUSSION

In this study, we investigated the persistence and expansion in patients of *in vitro* isolated and prophylactically infused multi-antigen virus-specific T-cell products in the presence or absence of viral reactivations by *in vivo* tracking of individual T-cell populations. In contrast to the pMHC-tetramer technology that we previously used(20), TCR sequencing of purified viral antigen-specific T-cell populations allowed us to identify multiple different clonal T-cell populations within the antigen-specific T-cell compartments. This permitted their tracking with high sensitivity and specificity in PB of patients after infusion of the virus-specific T-cell products. TCR-mapping of the donor-derived CMV-, EBV- and AdV-specific T cells in the products revealed the presence of medians of 30, 34, and 20 different TCR-sequences per product, respectively. This technology allowed us to follow the presence and kinetics of the virus-specific T cells after infusion into patients after alloSCT. It also made it possible to distinguish donor-derived virus-specific T cells that were already present in the patient before infusion from those exclusively derived from the infused T-cell products. TCR-sequences from the products that were exclusively found in PB after infusion of the products were documented in all patients infused with CMV-specific T cells, in 80% of patients infused with EBV-specific T cells and in 47% of patients infused with AdV-specific T cells. As expected, higher frequencies of TCRs identical to the T-cell products could be tracked in PB of patients with CMV or EBV reactivations, compared to patients without reactivations. Since only one patient experienced AdV reactivation, no conclusions could be drawn about the T-cell kinetics in the presence of this virus. All patients with CMV or EBV reactivations showed expansion of virus-specific TCRs with similar kinetics irrespective of the presence of some of these T cells in the patients prior to infusion, suggesting that the virus-specific T cells from the T-cell products indeed contributed to the antiviral immune response. Statistical modeling of the expansion/persistence kinetics of the adoptively transferred virus-specific T cells showed a significant correlation between the vigorous increase in the numbers of circulating product-derived CMV and EBV-specific T cells and viral-loads. In 100%, 67% and 50% of the patients infused with CMV-, EBV- or AdV- specific T cells, respectively, T cells with TCRs identical to those in infusion products could be tracked for extended periods, even in the absence of viral reactivations, indicating T-cell persistence and a potential role of the adoptively transferred T-cell products in long-term protection against viral reactivations.

Several phase I and phase II clinical studies have been performed exploring safety, feasibility and potential efficacy of adoptive transfer of *in vitro* selected virus-specific T-cell products derived from the original stem-cell donors to control refractory viral reactivations in patients following alloSCT(20, 30-34). Presence of virus-specific T cells in these patients was in some of these studies demonstrated using pMHC-tetramer-

based flow cytometry assays or ELIspot analysis. However, the origin of the detected virus-specific T cells could not be demonstrated using these assays. Similar studies have been performed in patients after solid organ transplantation that received autologous derived virus-specific T-cell products derived from the naïve T-cell repertoire (35). In this case, the origin of the virus-specific T cells that were observed in the patients was clear, but also in this study it remained difficult to unequivocally link the clinical effects to the infused T-cell product. In many cases, control of reactivation or even disappearance of clinical symptoms was documented after infusion of the virus-specific T cells(36, 37). However, even in case of (partial) T-cell depletion of the stem-cell grafts, virus-specific T cells that survive the T-cell depletion are co-administered with the graft and already present at the time of infusion of the T-cell product(28, 29). This makes it difficult to address whether the infused T-cell products were actually responsible for the clinical effects, despite a clear correlation between infusion of the cells and clinical benefit(32). With next-generation TCR sequencing techniques, adoptively transferred donor-derived T cells (e.g. virus-specific, tumor-specific or regulatory T cells) could be more efficiently tracked in peripheral blood samples of patients with virus-reactivations(38), organ transplantations(39), cancer(40) or auto-immune diseases(41). However, so far donor-derived virus-specific T cells were not yet tracked using TCR-sequences in patients that prophylactically received virus-specific T cells. By tracking many individual clonal virus-specific T-cell populations from the T-cell products and tracking them in patients clearing viral reactivations, we could demonstrate that the majority of T cells expanding in response to *in vivo* appearance of the virus were derived from the infused T-cell products. However, *de novo* generation of public TCRs in the recipient that originate from the donor-derived stem cells/naïve precursor T cells cannot be unequivocally excluded. Appearance of T cells expressing public TCRs are therefore difficult to link to the product. However, from previous studies we know that memory $CD8^{pos}$ T cells dominate the immune reconstitution at week 6 post alloSCT compared to naïve T cells. Also, naïve T cells are more efficiently depleted following alemtuzumab based T-cell depletion(28), making it less likely that such T cells expressing public TCRs emerging early after alloSCT would be derived from the naïve donor T-cell repertoire. Additionally, patient-derived virus-specific T cells can also contribute to the control of viral reactivations after alloSCT, especially after NMA TCD alloSCT as described previously (42). Since the focus within the current study was on the *in vivo* fate of donor-derived virus-specific T cells upon adoptive transfer rather than on the entire virus-specific immunity post-transplant, we did not quantify and annotate patient-derived virus-specific T cells and can therefore not elaborate on the role of the host immunity in these specific patients. Gene-edited donor-derived T-cells could circumvent part of this problem by tracking T cells with the inserted gene *in vivo*, thereby limiting the influence of autologous derived TCR-sequences(15, 43, 44). Long-term persistence was shown for adoptively transferred gene-marked EBV-specific T cells using this approach(15). It has been suggested that

co-infusion of virus-specific CD4$^{pos}$ and CD8$^{pos}$ T cells may be beneficial(45-47), our study also strongly supports previous indications that *in vitro* selection based on purification of virus-specific CD8$^{pos}$ T cells by peptide/MHC complexes using the Streptamer technology does not hamper the *in vivo* functionality of these cells after infusion(20), resulting in expansion and long-term persistence without the co-infusion of virus-specific CD4$^{pos}$ T cells. It was reported that the diversity of TCRs of CMV-specific T-cell populations reduces during viral-reactivations(48). However, in our analyses we did not observe any reduction in diversity of the TCR-repertoire, even in those patients where clonal expansion of virus-specific T-cell populations was overt. The high sequencing depth of our strategy allowed us to also detect persisting virus-specific T-cell clones that were not expanding, but that contributed to the diversity of the TCR-repertoire. Since our clinical phase I/II study(20) did not include a control arm without T-cell product infusion or placebo, we can not demonstrate the reconstitution and expansion kinetics in patients who did not receive adoptively transferred virus-specific T cells.

The strategy we applied to perform bulk TCR-beta sequencing of thousands of cells in parallel is a powerful tool to dissect the diversity of the TCR-repertoire of multiple T-cell populations. However, the main limit relies in the impossibility to pair the information regarding TCR-alpha and TCR-beta sequences of individual T cells. Paired single-cell sequencing of TCR-alpha and TCR-beta chains would have allowed us to provide information on the TCR-alpha usage of product-derived virus-specific T cells. However, single-cell sequencing is more limited in the number of cells that can be sequenced simultaneously, thereby losing resolution required for the detection of T-cell populations that are present at low frequencies in the peripheral blood samples of patients. This can potentially result in undetected donor-derived virus-specific T cells before infusion or undetected persisting virus-specific T cells when viral-loads are absent.

Although TCR-beta sequencing of product-derived virus-specific T-cell populations allowed for tracking of individual T-cell clones upon adoptive transfer to patients, it remains possible that TCRs of T cells from the patient contain exactly the same nucleotide sequence as the donor/product—derived TCRs. We recently demonstrated that the magnitude, defined as frequency and occurrence, of such public TCRs is high, but that this was only on the amino-acid level(26), illustrating that the majority of TCRs contained different nucleotide sequences as a results of convergent recombination and random nucleotide inserts between V-D-J regions. Therefore, the chance of shared TCR nucleotide sequences between patient and donor has been estimated to be relatively low.

The majority of studies exploring the potential benefit of *in vitro* selected virus-specific T cells has been performed in a preemptive or therapeutic setting. In these cases,

the cells are infused when viral reactivation already occurs in the patient. This does not allow evaluation of survival/persistence of the T-cell products when they do not immediately encounter their antigen *in vivo*. It has been suggested that under those circumstances survival of the adoptively transferred T cells may be poor. Obviously, in the absence of antigen and expansion, the contribution of the infused T cells to the total peripheral T-cell repertoire in the patient is generally too low to allow detection using the pMHC-tetramer technology(49). However, our approach allowed us to determine the *in vivo* persistence of prophylactically infused T-cell products even in the absence of viral reactivations. In the absence of viral reactivations, we found evidence that infused virus specific T cells persisted at very low frequencies without clear expansion. In a few patients we could also detect late expansion of these infused T cells, supporting the persistent functionality following *in vitro* selection and infusion of the virus-specific T-cell products even in the absence of direct *in vivo* antigen encounter. Statistical modeling of the expansion/persistence kinetics of the adoptively transferred virus-specific T cells showed a significant correlation between the vigorous increase in the numbers of circulating product-derived CMV and EBV-specific T cells and viral-loads. It could be assumed that different virus-specific T-cell populations targeting different antigens can have different efficacies, but modeling of the different CMV/EBV-specificities separately was not possible in our study due to the limited numbers and resulting insufficient power. However, as shown in figures 3 and 4, different virus-specific T-cell populations showed very similar expansion kinetics within each patient, assuming no large differences in efficacies between specificities.



In conclusion, our study shows that TCR sequencing allow highly sensitive and specific tracking and tracing of multiple clonal T-cell populations from *in vitro* selected donor-derived virus-specific $CD8^{pos}$ T-cell products, after infusion into patients after alloSCT. Using this methodology, we were able to distinguish expansion and persistence of virus-specific T-cell populations selectively derived from the infused T-cell products from those T cells that were already present in the patients prior to infusion. We demonstrated after viral reactivation *in vivo* expansion of multiple clonal T-cell populations from multi-virus-specific $CD8^{pos}$ T-cell products *in vitro* purified by the Streptamer technology. We showed persistence of prophylactically infused virus-specific T cells derived from the infused T-cell products in the absence of viral reactivation, illustrating long-term persistence. These results suggest that infusion of donor-derived multi-virus-specific T cells in a prophylactic setting early after T-cell depleted alloSCT may be a viable option to prevent viral complications.

**Acknowledgement**

This work was supported by Sanquin Research and Landsteiner Laboratory for Blood Cell research [PPO 15-37/Lnumber 2101]. This study was in part supported by research

funding from Stichting den Brinker (The Netherlands, Zeist). This study was additionally supported by the European Union's seventh Framework Program (FP/2007–2013) under grant agreement number 601722, by Dutch Cancer Society grant UL 2008-4263 and by German Cancer Society grant DFG-FOR 28030, project P09. These sponsors are nonprofit organizations that supports science in general. They had no role in gathering, analyzing, or interpreting the data.

# REFERENCES


1. Rohaan MW, Wilgenhof S, Haanen J. Adoptive cellular therapies: the current landscape. Virchows Arch. 2019;474(4):449-61.
2. Chapuis AG, Desmarais C, Emerson R, Schmitt TM, Shibuya K, Lai I, et al. Tracking the Fate and Origin of Clinically Relevant Adoptively Transferred CD8(+) T Cells In Vivo. Sci Immunol. 2017;2(8).
3. Cobbold M, Khan N, Pourgheysari B, Tauro S, McDonald D, Osman H, et al. Adoptive transfer of cytomegalovirus-specific CTL to stem cell transplant patients after selection by HLA-peptide tetramers. J Exp Med. 2005;202(3):379-86.
4. Feuchtinger T, Matthes-Martin S, Richard C, Lion T, Fuhrer M, Hamprecht K, et al. Safe adoptive transfer of virus-specific T-cell immunity for the treatment of systemic adenovirus infection after allogeneic stem cell transplantation. Br J Haematol. 2006;134(1):64-76.
5. Heslop HE, Rooney CM. Adoptive cellular immunotherapy for EBV lymphoproliferative disease. Immunol Rev. 1997;157:217-22.
6. Leen AM, Bollard CM, Mendizabal AM, Shpall EJ, Szabolcs P, Antin JH, et al. Multicenter study of banked third-party virus-specific T cells to treat severe viral infections after hematopoietic stem cell transplantation. Blood. 2013;121(26):5113-23.
7. Leen AM, Myers GD, Sili U, Huls MH, Weiss H, Leung KS, et al. Monoculture-derived T lymphocytes specific for multiple viruses expand and produce clinically relevant effects in immunocompromised individuals. Nat Med. 2006;12(10):1160-6.
8. Li Pira G, Kapp M, Manca F, Einsele H. Pathogen specific T-lymphocytes for the reconstitution of the immunocompromised host. Curr Opin Immunol. 2009;21(5):549-56.
9. Meij P, Jedema I, Zandvliet ML, van der Heiden PL, van de Meent M, van Egmond HM, et al. Effective treatment of refractory CMV reactivation after allogeneic stem cell transplantation with in vitro-generated CMV pp65-specific CD8+ T-cell lines. J Immunother. 2012;35(8):621-8.
10. O'Reilly RJ, Doubrovina E, Trivedi D, Hasan A, Kollen W, Koehne G. Adoptive transfer of antigen-specific T-cells of donor type for immunotherapy of viral infections following allogeneic hematopoietic cell transplants. Immunol Res. 2007;38(1-3):237-50.
11. Riddell SR, Watanabe KS, Goodrich JM, Li CR, Agha ME, Greenberg PD. Restoration of viral immunity in immunodeficient humans by the adoptive transfer of T cell clones. Science. 1992;257(5067):238-41.
12. Walter EA, Greenberg PD, Gilbert MJ, Finch RJ, Watanabe KS, Thomas ED, et al. Reconstitution of cellular immunity against cytomegalovirus in recipients of allogeneic bone marrow by transfer of T-cell clones from the donor. N Engl J Med. 1995;333(16):1038-44.
13. Slota M, Lim JB, Dang Y, Disis ML. ELISpot for measuring human immune responses to vaccines. Expert Rev Vaccines. 2011;10(3):299-306.
14. Roederer M. How many events is enough? Are you positive? Cytometry Part A. 2008;73A(5):384-5.
15. Heslop HE, Ng CY, Li C, Smith CA, Loftin SK, Krance RA, et al. Long-term restoration of immunity against Epstein-Barr virus infection by adoptive transfer of gene-modified virus-specific T lymphocytes. Nat Med. 1996;2(5):551-5.
16. Peggs KS, Verfuerth S, Pizzey A, Chow SL, Thomson K, Mackinnon S. Cytomegalovirus-specific T cell immunotherapy promotes restoration of durable functional antiviral immunity following allogeneic stem cell transplantation. Clin Infect Dis. 2009;49(12):1851-60.
17. Rosati E, Dowds CM, Liaskou E, Henriksen EKK, Karlsen TH, Franke A. Overview of methodologies for T-cell receptor repertoire analysis. BMC Biotechnol. 2017;17(1):61.
18. Einsele H, Roosnek E, Rufer N, Sinzger C, Riegler S, Loffler J, et al. Infusion of cytomegalovirus (CMV)-specific T cells for the treatment of CMV infection not responding to antiviral chemotherapy. Blood. 2002;99(11):3916-22.
19. Roex MCJ, Hageman L, Heemskerk MT, Veld SAJ, van Liempt E, Kester MGD, et al. The simultaneous isolation of multiple high and low frequent T-cell populations from donor peripheral blood mononuclear cells using the major histocompatibility complex I-Streptamer isolation technology. Cytotherapy. 2018;20(4):543-55.
20. Roex MCJ, van Balen P, Germeroth L, Hageman L, van Egmond E, Veld SAJ, et al. Generation and infusion of multi-antigen-specific T cells to prevent complications early after T-cell depleted allogeneic stem cell transplantation-a phase I/II study. Leukemia. 2020;34(3):831-44.
21. Garboczi DN, Hung DT, Wiley DC. HLA-A2-peptide complexes: refolding and crystallization of molecules expressed in Escherichia coli and complexed with single antigenic peptides. Proc Natl Acad Sci U S A. 1992;89(8):3429-33.
22. Rodenko B, Toebes M, Hadrup SR, van Esch WJ, Molenaar AM, Schumacher TN, et al. Generation of peptide-MHC class I complexes through UV-mediated ligand exchange. Nat Protoc. 2006;1(3):1120-32.
23. Eijsink C, Kester MG, Franke ME, Franken KL, Heemskerk MH, Claas FH, et al. Rapid assessment of the antigenic integrity of tetrameric HLA complexes by human monoclonal HLA antibodies. J Immunol Methods. 2006;315(1-2):153-61.
24. Koning MT, Nteleah V, Veelken H, Navarrete MA. Template-switching anchored polymerase chain reaction reliably amplifies functional lambda light chain transcripts of malignant lymphoma. Leuk Lymphoma. 2014;55(5):1212-4.
25. van Bergen CA, van Luxemburg-Heijs SA, de

Wreede LC, Eefting M, von dem Borne PA, van Balen P, et al. Selective graft-versus-leukemia depends on magnitude and diversity of the alloreactive T cell response. J Clin Invest. 2017;127(2):517-29.
26. Huisman W, Hageman L, Leboux DAT, Khmelevskaya A, Efimov GA, Roex MCJ, et al. Public T-Cell Receptors (TCRs) Revisited by Analysis of the Magnitude of Identical and Highly-Similar TCRs in Virus-Specific T-Cell Repertoires of Healthy Individuals. Frontiers in Immunology. 2022;13.
27. Bolotin DA, Poslavsky S, Mitrophanov I, Shugay M, Mamedov IZ, Putintseva EV, et al. MiXCR: software for comprehensive adaptive immunity profiling. Nat Methods. 2015;12(5):380-1.
28. Roex MCJ, Wijnands C, Veld SAJ, van Egmond E, Bogers L, Zwaginga JJ, et al. Effect of alemtuzumab-based T-cell depletion on graft compositional change in vitro and immune reconstitution early after allogeneic stem cell transplantation. Cytotherapy. 2021;23(1):46-56.
29. Loeff FC, Falkenburg JHF, Hageman L, Huisman W, Veld SAJ, van Egmond HME, et al. High Mutation Frequency of the PIGA Gene in T Cells Results in Reconstitution of GPI Anchor(-)/CD52(-) T Cells That Can Give Early Immune Protection after Alemtuzumab-Based T Cell-Depleted Allogeneic Stem Cell Transplantation. J Immunol. 2018;200(6):2199-208.
30. Blyth E, Clancy L, Simms R, Ma CK, Burgess J, Deo S, et al. Donor-derived CMV-specific T cells reduce the requirement for CMV-directed pharmacotherapy after allogeneic stem cell transplantation. Blood. 2013;121(18):3745-58.
31. Feuchtinger T, Opherk K, Bethge WA, Topp MS, Schuster FR, Weissinger EM, et al. Adoptive transfer of pp65-specific T cells for the treatment of chemorefractory cytomegalovirus disease or reactivation after haploidentical and matched unrelated stem cell transplantation. Blood. 2010;116(20):4360-7.
32. Gerdemann U, Katari UL, Papadopoulou A, Keirnan JM, Craddock JA, Liu H, et al. Safety and clinical efficacy of rapidly-generated trivirus-directed T cells as treatment for adenovirus, EBV, and CMV infections after allogeneic hematopoietic stem cell transplant. Mol Ther. 2013;21(11):2113-21.
33. Koehne G, Hasan A, Doubrovina E, Prockop S, Tyler E, Wasilewski G, et al. Immunotherapy with Donor T Cells Sensitized with Overlapping Pentadecapeptides for Treatment of Persistent Cytomegalovirus Infection or Viremia. Biol Blood Marrow Transplant. 2015;21(9):1663-78.
34. Ma CK, Blyth E, Clancy L, Simms R, Burgess J, Brown R, et al. Addition of varicella zoster virus-specific T cells to cytomegalovirus, Epstein-Barr virus and adenovirus tri-specific T cells as adoptive immunotherapy in patients undergoing allogeneic hematopoietic stem cell transplantation. Cytotherapy. 2015;17(10):1406-20.
35. Smith C, Beagley L, Rehan S, Neller MA, Crooks P, Solomon M, et al. Autologous Adoptive T-cell Therapy for Recurrent or Drug-resistant Cytomegalovirus Complications in Solid Organ Transplant Recipients: A Single-arm Open-label Phase I Clinical Trial. Clin Infect Dis. 2019;68(4):632-40.
36. Papadopoulou A, Gerdemann U, Katari UL, Tzannou I, Liu H, Martinez C, et al. Activity of broad-spectrum T cells as treatment for AdV, EBV, CMV, BKV, and HHV6 infections after HSCT. Sci Transl Med. 2014;6(242):242ra83.
37. Meij P, Jedema I, Zandvliet ML, van der Heiden PLJ, van de Meent M, van Egmond HME, et al. Effective Treatment of Refractory CMV Reactivation After Allogeneic Stem Cell Transplantation With In Vitro-generated CMV pp65-specific CD8(+) T-cell Lines. J Immunother. 2012;35(8):621-8.
38. Keller MD, Darko S, Lang H, Ransier A, Lazarski CA, Wang Y, et al. T-cell receptor sequencing demonstrates persistence of virus-specific T cells after antiviral immunotherapy. Br J Haematol. 2019;187(2):206-18.
39. Dziubianau M, Hecht J, Kuchenbecker L, Sattler A, Stervbo U, Rodelsperger C, et al. TCR repertoire analysis by next generation sequencing allows complex differential diagnosis of T cell-related pathology. Am J Transplant. 2013;13(11):2842-54.
40. Thiel U, Schober SJ, Einspieler I, Kirschner A, Thiede M, Schirmer D, et al. Ewing sarcoma partial regression without GvHD by chondromodulin-I/HLA-A*02:01-specific allorestricted T cell receptor transgenic T cells. Oncoimmunology. 2017;6(5).
41. Theil A, Wilhelm C, Kuhn M, Petzold A, Tuve S, Oelschlagel U, et al. T cell receptor repertoires after adoptive transfer of expanded allogeneic regulatory T cells. Clin Exp Immunol. 2017;187(2):316-24.
42. Sellar RS, Vargas FA, Henry JY, Verfuerth S, Charrot S, Beaton B, et al. CMV promotes recipient T-cell immunity following reduced-intensity T-cell-depleted HSCT, significantly modulating chimerism status. Blood. 2015;125(4):731-9.
43. Biasco L, Scala S, Basso Ricci L, Dionisio F, Baricordi C, Calabria A, et al. In vivo tracking of T cells in humans unveils decade-long survival and activity of genetically modified T memory stem cells. Sci Transl Med. 2015;7(273):273ra13.
44. Morgan RA, Dudley ME, Wunderlich JR, Hughes MS, Yang JC, Sherry RM, et al. Cancer regression in patients after transfer of genetically engineered lymphocytes. Science. 2006;314(5796):126-9.
45. Peggs KS, Thomson K, Samuel E, Dyer G, Armoogum J, Chakraverty R, et al. Directly selected cytomegalovirus-reactive donor T cells confer rapid and safe systemic reconstitution of virus-specific immunity following stem cell transplantation. Clin Infect Dis. 2011;52(1):49-57.
46. Foster AE, Gottlieb DJ, Sartor M, Hertzberg MS, Bradstock KF. Cytomegalovirus-specific CD4+ and CD8+ T-cells follow a similar reconstitution pattern after allogeneic stem cell transplantation. Biol Blood Marrow Transplant. 2002;8(9):501-11.

47. Bollard CM, Heslop HE. T cells for viral infections after allogeneic hematopoietic stem cell transplant. Blood. 2016;127(26):3331-40.
48. Wang GC, Dash P, McCullers JA, Doherty PC, Thomas PG. T cell receptor αβ diversity inversely correlates with pathogen-specific antibody levels in human cytomegalovirus infection. Sci Transl Med. 2012;4(128):128ra42.
49. Dolton G, Zervoudi E, Rius C, Wall A, Thomas HL, Fuller A, et al. Optimized Peptide-MHC Multimer Protocols for Detection and Isolation of Autoimmune T-Cells. Front Immunol. 2018;9:1378.

**Supplementary Table 1. Patient and transplantation characteristics.**

| Patient | Diagnosis | Graft type | Condit-ioning regimen | Anti-viral medication | TCD *in vivo* | TCD *in vitro* | CMV serostatus patient/donor | EBV serostatus patient/donor | HLA-matching |
|---|---|---|---|---|---|---|---|---|---|
| 3 | MM | unrelated | NMA | No | ALM+ATG | ALM | neg/neg | pos/pos | 10/10 |
| 4 | MM | related | NMA | No | ALM | ALM | neg/pos | neg/pos | 12/12 |
| 7 | AML | unrelated | MA | No | ALM | ALM | pos/pos | pos/pos | 10/10 |
| 8 | AML | unrelated | NMA | CMV: VAL T=70 days EBV: RIT+PRED T=62 days | ALM+ATG | ALM | pos/neg | pos/pos | 10/10 |
| 10 | MM | related | NMA | No | ALM | ALM | pos/neg | pos/pos | 12/12 |
| 11 | MM | unrelated | NMA | CMV: VAL T=0 | ALM+ATG | ALM | pos/pos | pos/pos | 10/10 |
| 13 | MM | unrelated | NMA | No | ALM+ATG | ALM | pos/pos | pos/pos | 10/10 |
| 14 | MM | related | NMA | No | ALM | ALM | pos/neg | pos/pos | 12/12 |
| 15 | MCL | related | NMA | No | ALM | ALM | pos/neg | pos/pos | 12/12 |
| 16 | AML | unrelated | NMA | No | ALM+ATG | ALM | pos/pos | pos/pos | 10/10 |
| 17 | MM | unrelated | NMA | No | ALM+ATG | ALM | neg/pos | pos/pos | 9/10 |
| 18 | AML | unrelated | NMA | No | ALM+ATG | ALM | neg/neg | pos/pos | 10/10 |
| 20 | AML | unrelated | MA | No | ALM | ALM | neg/neg | pos/pos | 10/10 |
| 21 | AML | related | MA | No | *No TCD* | ALM | neg/pos | pos/pos | 12/12 |
| 22 | AML | unrelated | MA | CMV: GAN T=14 days | ALM | ALM | pos/pos | pos/pos | 10/10 |
| 23 | AML | related | MA | No | *No TCD* | ALM | neg/pos | pos/pos | 12/12 |
| 24 | B-ALL | unrelated | MA | CMV: VAL T=0 | ALM | ALM | pos/pos | pos/pos | 9/10 |
| 25 | Myelo-fibrosis | related | NMA | No | ALM | ALM | neg/pos | pos/pos | 12/12 |
| 26 | LPL | unrelated | NMA | No | ALM+ATG | ALM | pos/pos | pos/pos | 10/10 |
| 27 | MDS | unrelated | NMA | CMV: VAL T=0 and T=30 days | ALM+ATG | ALM | pos/pos | pos/pos | 10/10 |

Table adapted from Supplementary Table 3 from the publication by Roex et al, describing the results of the clinical phase I/II study[4]. ALL, acute lymphoblastic leukemia; AML, acute myeloid leukemia; LPL, lymphoplasmacytic lymphoma; MA, myeloablative; MCL, mantle cell lymphoma; MDS, myelodysplastic syndrome; neg, negative; pos, positive; NMA, non-myeloablative; TCD, T-cell depletion; ALM, Alemtuzumab; ATG, Anti-Thymocyte Globulin.; VAL, valganciclavir; GAN, ganciclovir; RIT+PRED, Rituximab + prednisolone; T=0, anti-viral medication before and at moment of infusion of T-cell product; T=>0, day start of medication after T-cell product infusion

**Supplementary Table 2. Primer sequences.**

| Description | Name | Nucleotide sequence 5'►3' |
|---|---|---|
| cDNA primer TRB constant region reverse transcription | TRB_RT | CACGTGGTCGGGGWAGAAGC |
| cDNA primer SmartSeq2modified template switching oligo | SS2m_TSO | AAGCAGTGGTATCAACGCAGAGTACAT(G)(G){G} |
| PCR primer SmartSeq2modified forward | SS2m_For | GAGTTCAGACGTGTGCTCTTCCGATCTAAGCAGTGGTATCAACGCAGAGTACAT*G |
| PCR primer TRBC1 reverse | TRBC1_rev | CCTACACGACGCTCTTCCGATCTGTGGGAACACCTTGTTCAGGTCCT*C |
| PCR primer TRBC1 reverse | TRBC2_rev | CCTACACGACGCTCTTCCGATCTGTGGGAACACGTTTTTCAGGTCCT*C |
| Barcode primer SS2m region, forward, backbone | BC_R7xx_For | CAAGCAGAAGACGGCATACGAGAT$_{nnnnnn}$GTGACTGGAGTTCAGACGTGTGCTCTTCCGAT*C |
| Barcode primer TRBC region reverse, backbone | BC_R7xx_Rev | AATGATACGGCGACCACCGAGATCTACAC$_{nnnnnn}$ACACTCTTTCCCTACACGACGCTCTTCCGATC*T |

Abbreviations: TRB: T-cell Receptor Beta, SS2m: SmartSeq2Modified, TSO: Template Switching Oligo, TRBC: T-cell Receptor Beta Constant, For: Forward, Rev: Reverse, BC: Beta chain, nnnnnn: Identifier sequence
()=RNA, {}=LNA: Locked Nucleic Acid, *:phosphonothioate-binding

**Supplementary Table 3. Identifier sequences.**

| Identifiers (For) Name | Identifiers (For) Seq | Identifiers (Rev) Name | Identifiers (Rev) Seq |
|---|---|---|---|
| BC_R701 | ATCACG | BC_R725 | ACTGAT |
| BC_R702 | CGATGT | BC_R726 | ATGAGC |
| BC_R703 | TTAGGC | BC_R727 | ATTCCT |
| BC_R704 | TGACCA | BC_R728 | CAAAAG |
| BC_R705 | ACAGTG | BC_R729 | CAACTA |
| BC_R706 | GCCAAT | BC_R730 | CACCGG |
| BC_R707 | CAGATC | BC_R731 | CACGAT |
| BC_R708 | ACTTGA | BC_R732 | CACTCA |
| BC_R709 | GATCAG | BC_R733 | CAGGCG |
| BC_R710 | TAGCTT | BC_R734 | CATGGC |
| BC_R711 | GGCTAC | BC_R735 | CATTTT |
| BC_R712 | CTTGTA | BC_R736 | CCAACA |
| BC_R713 | AGTCAA | BC_R737 | CGGAAT |
| BC_R714 | AGTTCC | BC_R738 | CTAGCT |
| BC_R715 | ATGTCA | BC_R739 | CTATAC |
| BC_R716 | CCGTCC | BC_R740 | CTCAGA |
| BC_R717 | GTAGAG | BC_R741 | GACGAC |
| BC_R718 | GTCCGC | BC_R742 | TAATCG |
| BC_R719 | GTGAAA | BC_R743 | TACAGC |
| BC_R720 | GTGGCC | BC_R744 | TATAAT |
| BC_R721 | GTTTCG | BC_R745 | TCATTC |
| BC_R722 | CGTACG | BC_R746 | TCCCGA |
| BC_R723 | GAGTGG | BC_R747 | TCGAAG |
| BC_R724 | GGTAGC | BC_R748 | TCGGCA |

Unique molecular identifiers were used per sample from one patient. Sequencing was performed per patient allowing up to 24 different samples that could be barcoded with unique identifiers.

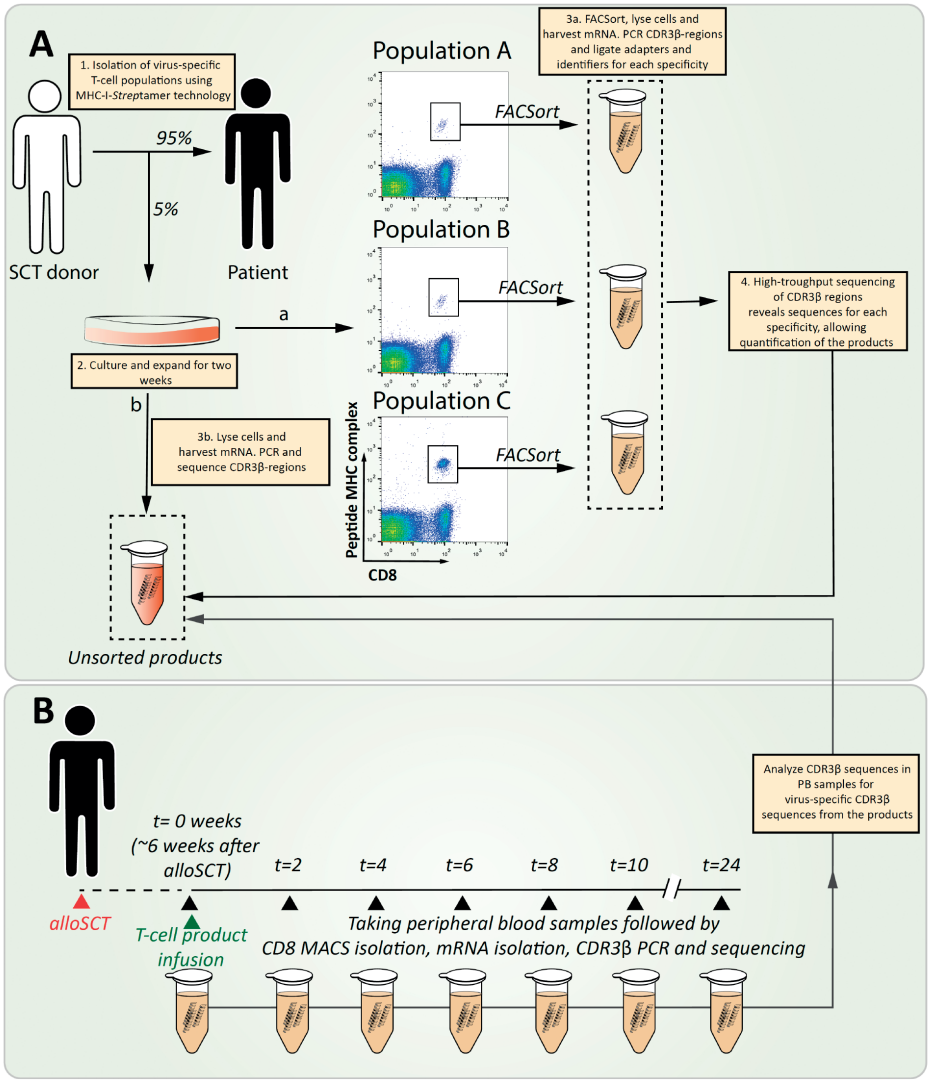


**Supplementary Figure 1. Schematic overview of high-throughput sequencing of the T-cell receptors of T cells from virus-specific T-cell products. A)** T cells from 20 products were successfully expanded *in vitro*. Virus-specific T-cell populations that target a single antigen were then isolated from the cultured products and mRNA was harvested directly after FACSort. Unique identifiers were ligated to the PCR products for each T-cell population. The remainders of the unsorted products were additionally sequenced to quantify the different TCR-nucleotide sequences (CDR3β-sequences) present within the T-cell products. **B)** PBMCs were isolated from PB of patients drawn before (day 0) and after infusion of the T-cell products. PB samples were collected every ~2 weeks followed by PBMC selection, CD8 MACS isolation, mRNA isolation and sequencing of the TCRs. CDR3β-sequences from these monitoring samples were compared with the CDR3β-sequences from the products.
Abbreviations: alloSCT, allogeneic stem cell transplantation. MACS, magnetic activated cell sorting. SCT, stem cell transplantation. FACS, Fluorescence activated cell sorting. CDR3, complementary determining region 3. MHC, major histocompatibility complex.

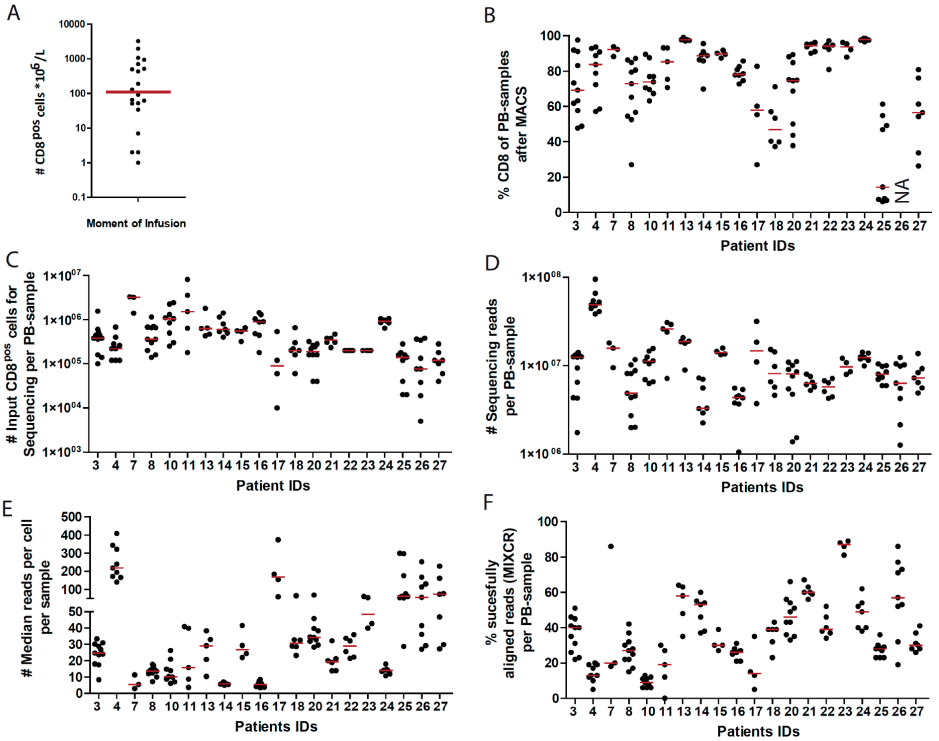


**Supplementary Figure 2. Sample quality assessment of peripheral blood samples of patients. A)** The absolute numbers of $CD8^{pos}$ T cells are shown for each patient at moment of product infusion **B**) The CD8 purity after CD8 Magnetic Activated Cell Sorted (MACS) per peripheral blood sample is shown for each patient. **C**) The number of CD8 MACSorted T cells used as input for TCR-beta sequencing are shown per peripheral blood sample for each patient. **D**) The total number of TCR sequencing reads for each CD8 MACSorted peripheral blood sample are shown for each patient. (**E**) The median number of TCR sequencing reads per cell are shown per sample for each patient. **F**) The percentage of reads that could successfully be aligned using MIXCR are shown per sample for each patient.
Red lines indicate medians.NA, not available

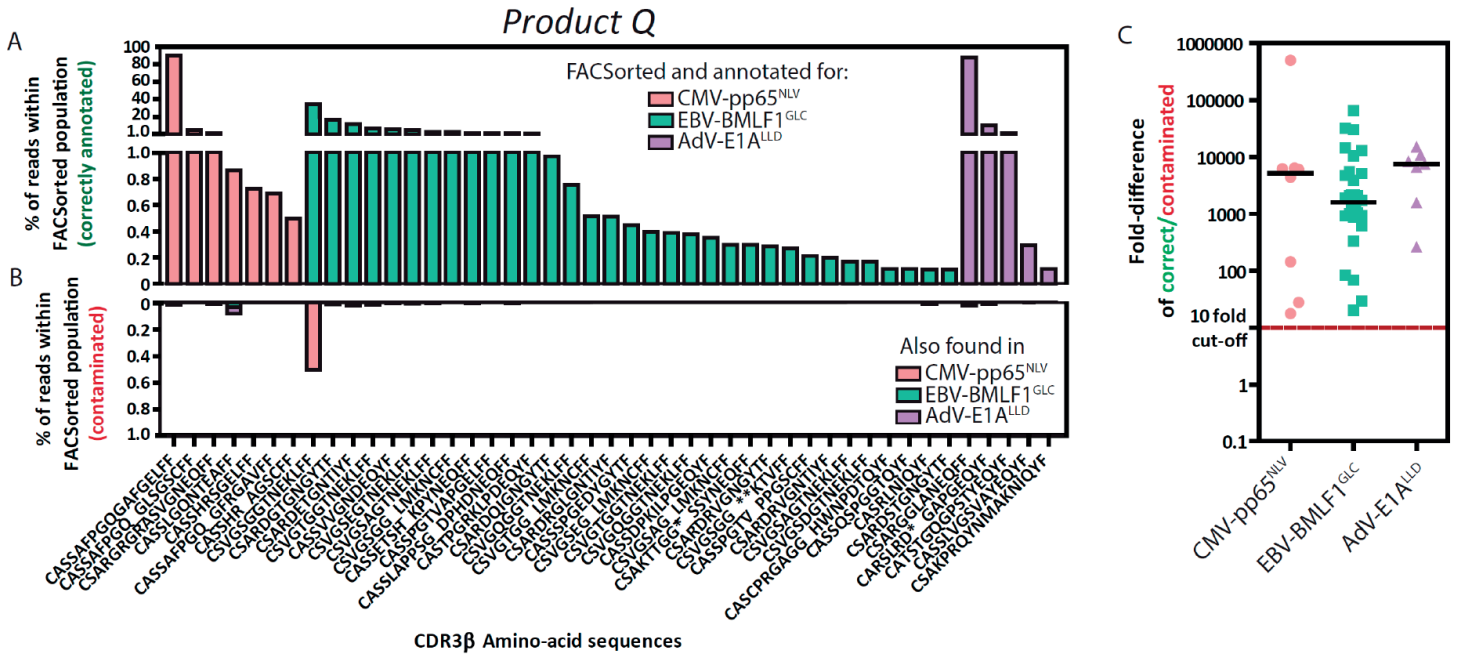


**Supplementary Figure 3. Overlap of TCR-CDR3β sequences between FACSorted specificities**. A representative example is shown of FACSorted virus-specific T-cell populations from product Q. A) The percentages of TCR-CDR3β sequences that were present in each of the FACSorted virus-specific T-cell populations are shown on the y-axis. B) The percentages are shown of TCR-CDR3β sequences that were also detected in another FACSorted virus-specific T-cell population (contamination). C) A cut-off fold-difference of 10-fold between the % of sequences annotated to the correct specificity and the % of contamination in another sample was used to determine correct annotation of TCR-CDR3β sequences to the corresponding specificity.

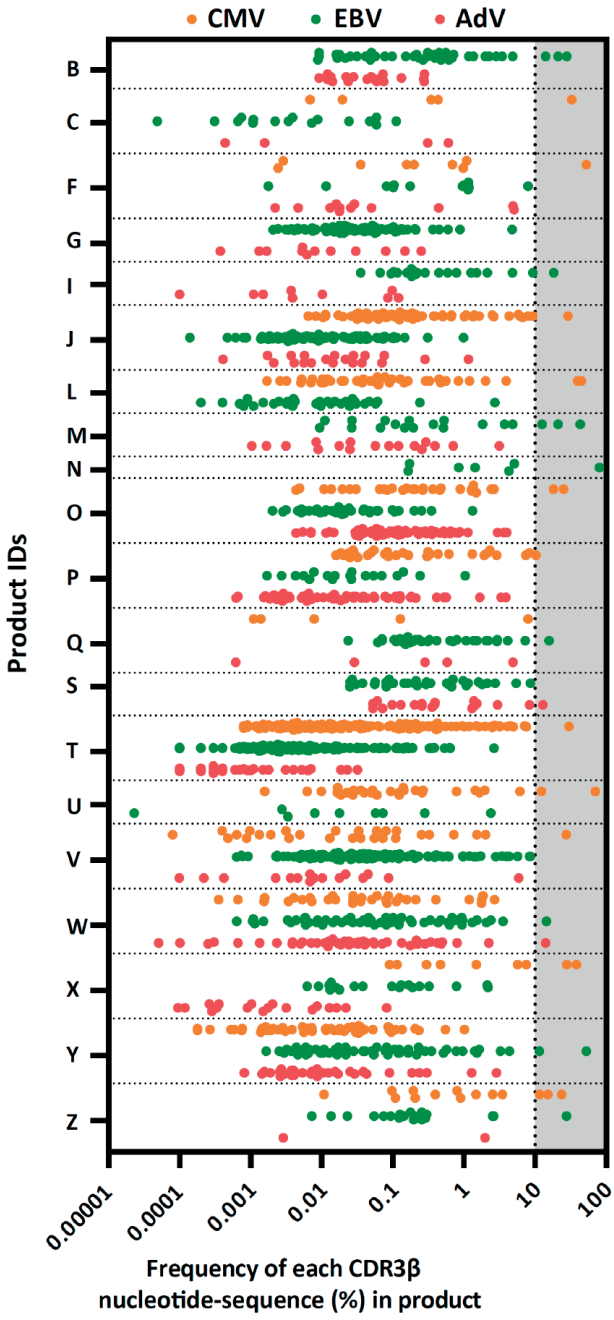


**Supplementary Figure 4. Frequencies of CMV, EBV and AdV-specific TCR-nucleotide sequences within each product.** Shown are the frequencies (number of specific CDR3β-sequence reads as a proportion of the total number of CDR3β-sequence reads) of different CMV, EBV or AdV-specific TCR-nucleotide sequences (CDR3β-sequences) within each product. Each dot represents the frequency of a single CDR3β-sequence)

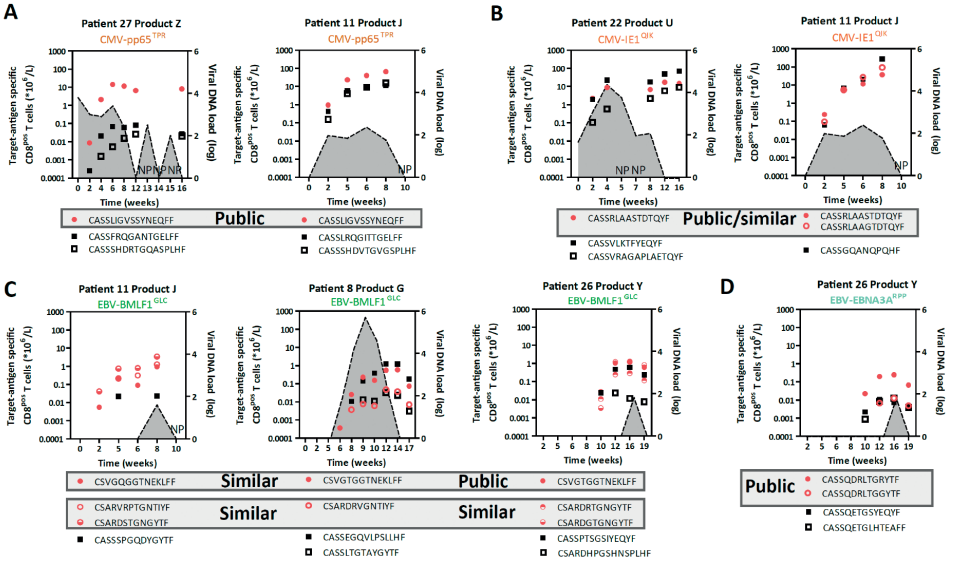


**Supplementary Figure 5. Tracking of public and private virus-specific T-cell clones that appeared only after infusion of the T-cell product**. Representative examples are shown of T-cell products that contained virus-specific T-cell populations with public TCRs or TCRs that were highly-similar to public TCRs. The virus-specific T-cell clones from these examples were only detected in the patient after infusion of the product. Viral DNA loads are shown as filled grey areas. **A** and **B**). Two different CMV-specific T-cell populations were tracked in three patients that contained a CMV-pp65$^{TPR}$-specific public TCR (red, A) and a CMV-IE1$^{QIK}$-specific public TCR (red, B). Expansion kinetics of virus-specific T-cell clones that expressed private TCRs is shown in black rectangles. **C** and **D**) Two different EBV-specific T-cell populations were tracked in three patients that contained an EBV-BMLF1$^{GLC}$-specific public TCR (red, C) and an EBV-EBNA3A$^{RPP}$-specific public TCR (red, D). Expansion kinetics of T-cell clones with TCRs that are highly-similar to the published public TCR is shown as open red circles. Expansion kinetics of T-cell clones that express private TCRs is shown as black rectangles.
NP; Sequencing not performed.